

# Controlling the cross-section of waveguides inscribed on bulk chalcogenide glasses using fast laser

TAMILARASAN SABAPATHY<sup>a</sup>, GAYATHRI SIVAKUMAR<sup>a</sup>, ARUNBABU AYIRIVEETIL<sup>a</sup>, AJOY K. KAR<sup>b</sup>, SUNDARRAJAN ASOKAN<sup>a,b,c,d,\*</sup>

<sup>a</sup> Department of Instrumentation and Applied Physics, Institute of Science, Bangalore- 560 012, India

<sup>b</sup> School of Engineering and Physical Sciences, Heriot-Watt University, Edinburgh EH14 4AS, United Kingdom

<sup>c</sup> Applied Photonics Initiative, Institute of Science, Bangalore- 560 012, India

<sup>d</sup> Robert Bosch Centre for Cyber Physical Systems, Indian Institute of Science, Bangalore- 560 012, India

Waveguides have been fabricated on melt-quenched, bulk chalcogenide glasses using the femto-second laser inscription technique at low repetition rates in the single scan regime. The inscribed waveguides have been characterized by butt-coupling method and the diameter of the waveguide calculated using the mode-field image of the waveguide. The waveguide cross-section symmetry is analyzed using the heat diffusion model by relating the energy and translation speed of the laser. The net-fluence and symmetry of the waveguides are correlated based on the theoretical values and experimental results of guiding cross-section.

(Received August 14, 2013; accepted November 13, 2014)

*Keywords:* Integrated optics devices, Laser materials processing and Chalcogenide glasses

## 1. Introduction

Exposing chalcogenide glasses to radiation of appropriate energy bring about changes in many properties including refractive index of the material. Photo induced effects exhibited by glassy chalcogenides make them suitable for making devices for photonic applications. Chalcogenide glasses are also technologically important because of their interesting properties such as wide range of transparency from visible to infrared [1], high third order non-linearity ( $\chi^3$  which is about 1000 times great than that of silica), easiness to dope with rare earth ions, low phonon energy, etc. [2-4]. They are also attractive as their properties can be widely varied by varying the chemical composition. In addition, chalcogenide glasses are also chemically and thermally stable.

Ultrafast laser inscription (ULI) techniques for fabricating photonics integrated devices are receiving great interest because they are less complex compared to the lithographic techniques involving the clean room facility [5]. The ULI methods are based on multi-photon absorption induced by focusing sub band-gap energy on the material to produce high energy to modify its physical properties; it can be used for fabricating photonic devices such as waveguides [6], amplifiers [7] and lasers [8] on bulk dielectric transparent materials. By varying the focal point of the laser beam, multiple layers of waveguides in 3-dimension can be formed to fabricate high density photonic devices in a single substrate [9].

An optical waveguide's most defining property is the refractive index profile, or cross-section which directly determines the number of transverse modes supported by the waveguide, and the properties of the modes. These

properties directly affect the performance of the waveguide. Furthermore, asymmetric core shaped waveguides exhibit polarisation dependent guiding properties and increased coupling losses. Therefore, steps must be taken for appropriate control of spatial distribution of the refractive index modification induced by the inscription process, to create waveguides with optimum performance using the ultrafast laser inscription.

There are different techniques available for controlling the cross section of ultrafast laser inscribed waveguides, namely astigmatic beam shaping, slit-beam shaping, active optics and spatio-temporal focussing techniques [10-15]. The techniques mentioned above which use the single scan method, mostly involve complex designs to shape the laser beam to control the waveguide cross-section. The multi-scan technique is used to control the cross-section by scanning the substrate through the focus by many times to build the required waveguide cross-section.

In this work, we report the fabrication of buried channel waveguides on chalcogenide glass using ULI technique. As mentioned, the waveguide cross-section plays a vital role in guiding light, mode structure and coupling efficiency of the waveguide; controlling the structure helps to couple the device with standard telecommunication fibers and other commercial photonic devices. In this context, a heat diffusion model is used for controlling the waveguide cross-section and the theoretical results are compared with the experimental guiding cross-section.

## 2. Experimental

### 2.1 Fabrication and characterization

The waveguides are fabricated on GeGaS glasses of 5 mm length using the ULI technique with IMRA  $\mu$ jewel Laser (D400). The pulse duration is set to 350 fs at full-width half maximum points and a circular polarization is maintained. The central wavelength of the laser is 1047 nm at 100 kHz repetition rate. The waveguides have been inscribed 100  $\mu$ m below the surface by focusing the laser pulse train on the material using an aspheric lens with a numerical aperture (NA) of 0.67. The waveguides are separated by 50  $\mu$ m to avoid the stress influence and overlapping on the subsequent waveguide. The laser powers are tuned from 276 mW to 62 mW (by 95% step down) with translation speed of 1 mm/s, 2 mm/s, 3 mm/s, 4 mm/s and 6 mm/s; overlapping pulses of 99%, 98%, 97%, 96% and 94% have been used to inscribe the waveguides. The scanning method adopted here is the transverse geometry wherein the laser beam is focussed on the material and the sample is scanned perpendicular to the laser propagation direction. This scanning technique suffers from the disadvantage of the asymmetry in the waveguide cross-section [16] which induces a coupling loss [17]. The asymmetry arises because of the difference between the beam waist  $2\omega_0$  (which is in order of micrometres) and the confocal parameter  $b = 2\pi\omega_0^2/\lambda$  (which is approximately 100 times larger than the beam waist) [18, 19]. The longitudinal geometry can be used to overcome this problem; however, the inscription length is limited by working distance of the objective lens. The waveguide geometry also depends on the pulse duration, pulse energy and writing speed [20].

After the fabrication, the waveguides facets are grounded and subsequently polished to optical quality to remove any tapering effect in the waveguide closer to the edges. The waveguide near field image at 1550 nm wavelength is captured using an IR camera with 0.65 NA objective lens and the optically induced structure are captured with the help of an optical microscope with 50x magnification. The optical microscope image and near field image are shown in Fig. 1 (a) and (b) respectively. Fig. 1 (a) shows the asymmetry in the laser induced structural changes using the transverse geometry. The cross-section of the waveguide shows an elliptical ring around the focal volume extending from the beam focus towards the surface of the sample in an inverted tear-drop shape.



Fig. 1. (a) The optical microscopic image of single mode waveguide structure with 50x magnification under white light illumination and (b) its corresponding near field image at 1550 nm wavelength.

### 2.2 Effect of irradiation on shape of the waveguides

Chalcogenide glasses are optically highly non-linear in nature and exhibit multi-photon absorption [22]. This intrinsic property of the glass affects the dynamics of the beam immediately as it enters the material.

In the model used, it is assumed that above the glass transition temperature ( $T_g$ ) optical properties of glass vary due to irradiation, as a consequence of structural modifications [18, 22] within the modified region in the bulk transparent dielectric material. The numerical aperture of the focused beam used for writing waveguides is 1.2 (NA), which can also be accounted for determining the shape of modified region under irradiation with the low repetition rate of 100 kHz. Tightly focusing the beam using an objective with  $NA > 0.04$  at the focal region of the transparent glass, a drop like plasma region is formed and hence drop-shaped modification is produced [23].

Highly non-uniform cooling rates are attained due to variable temperatures across the modified zone [24], resulting in a non-uniform distribution in the density of the glass [25] which in turn changes the refractive index. The depth of the small, dark spot near the bottom of the structures (Fig. 2) is observed to be independent of average power (62 to 85 mW), repetition rate (100 KHz), and writing speed (1 to 4 mm/s). With reduced scan speed, the modified zones expands upwards towards the surface; however, the dark focal spot remains at the same depth, showing no evidence of self focusing [22]. More narrow and elongated structures can be expected [26] and are obtained at 100 kHz repetition rate. It can be seen that despite the ellipticity, the mode profile at 1550 nm is almost circular, as shown in Fig. 2.

In this work, we have studied the process of modifications by the femto-second laser beam under different irradiation conditions, which allowed us to understand the basic effects which determine the shape and size of the region modified under irradiation at low repetition rates.

At small times after irradiation, the region with  $T > T_g$  has a characteristic drop-like shape [27]. In the trailing edge of the pulse ( $\tau > 0$ ), the transverse distribution of the beam intensity adopts the shape of a ring, as upon non-linear absorption, the electron density “ $\rho$ ” increases from the leading to the trailing edge of the pulse. Therefore, the

trailing edge of the pulse is intensively absorbed and defocused.

This effect is strongly pronounced at the centre of the beam, whereas, at the periphery, the nonlinear absorption is practically absent. The drop like shape of the modified region is retained over a wide range of powers. Further, the decrease in the multi-photon absorption with decreasing beam intensity leads to a characteristic narrowing of the modified region in the direction towards the cold focus. In chalcogenide glasses, the longitudinal size of the modified region is considerably greater than in fused silica [22].

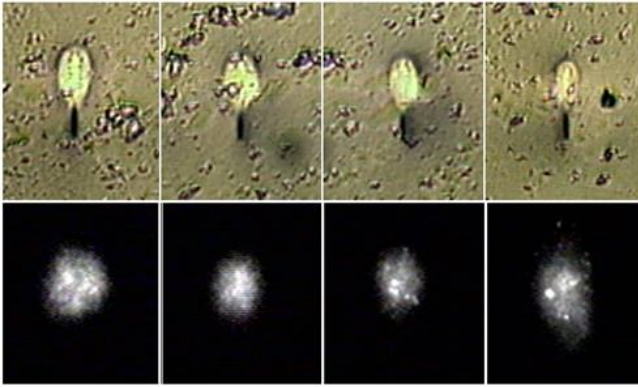


Fig. 2. Comparison of microscopic images and near field images of waveguides fabricated in GeGaS glass with 623nJ incident energy with 1mm/s, 2mm/s, 3 mm/s and 4 mm/s scan speeds.

### 2.3 Thermal diffusion model

A finite-difference thermal diffusion model [27-29] has been used to study the waveguide spatial formation in ultrafast laser inscribed GeGaS glass. The thermal distribution during the waveguide formation has been calculated with the heat diffusion model.

$$\frac{\partial}{\partial r} \left( r^2 \frac{\partial T}{\partial r} \right) = \frac{r^2}{D} \left( \frac{\partial T}{\partial t} \right) \quad (1)$$

The laser dissipation is treated as a spherical Gaussian distribution with an energy volume density  $E(r) = E_0 \exp(-r^2/w_0^2)$  with beam waist  $w_0$  set to the  $1/e^2$  radius of the focused laser beam waist.

The value of  $E_0$  depends on the absorbed laser pulse energy, which is inferred from measurement of the transmitted laser power. The values of  $E_0$  are varied by changing the laser power, scan speed and repetition rate. The temperature profile is augmented by an instantaneous temperature rise  $T(r) = E(r)/C_p \rho$ , during the continuous shot of laser pulse train. In order to model the effect of net-fluence during the waveguide inscription, the material parameters like Specific heat capacity  $C_p$ , thermal diffusivity  $D$  and density  $\rho$  should be known. The above mentioned parameters  $C_p = 673 \text{ J/kg.K}$ ,  $D = 0.0026 \text{ cm}^2/\text{s}$  and  $\rho = 2761.1 \text{ kg/m}^3$  of the material have been obtained in the present work, using modulated Alternative Differential Scanning Calorimetry (ADSC), a custom made photo-

thermal diffusivity instrument and Metler Toledo density Kit respectively.

At 100 kHz repetition rate, at the focal region the photo-induced temperature rise relaxes below the glass transition temperature before the next pulse arrives and significant diffusive cooling occurs. Hence, the thermal diffusion acts alone in determining the waveguide diameter. The strong laser-induced temperature rise within laser spot builds on top of a slowly building Gaussian heat distribution, yielding a melted volume which expands to sizes much larger than the spot size as further laser pulses are absorbed.

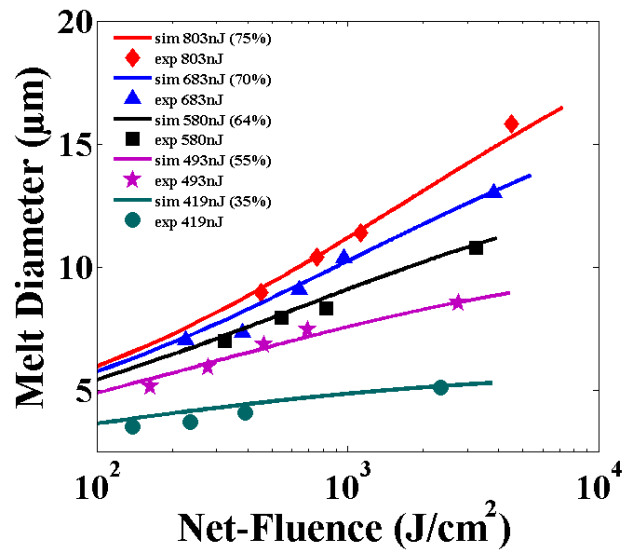


Fig. 3. The relation between the net-fluence versus experimentally calculated melt diameter and the theoretical melt diameter.

### 3. Results

Fig. 3 shows the relation between the net-fluence and the diameter of the waveguide from solving the thermal diffusion equation. NF were calculated using the relation,  $NF = 2\omega_0 R F_p / v$ , where  $2\omega_0$  is the laser spot size,  $R$  is the repetition rate  $v$  is the writing speed;  $F_p = E_p / \pi\omega_0^2$  is the fluence per pulse, and  $E_p$  is the incident laser pulse energy. On simplification, we get the net fluence,

$$NF = \frac{2R}{\pi\omega_0} \left( \frac{E_p}{v} \right) \quad (2)$$

We have chosen different energies with four different translation speeds for the modelling. The model best fits the experimental data, with 35%, 55%, 64%, 70% and 75% absorption for 419, 493, 508, 683 and 803 nJ of incident pulse energies respectively and the corresponding absorbed energies are 146 nJ, 271 nJ, 325 nJ, 478 nJ and 602 nJ respectively. This suggests that with increase in incident pulse energy the absorption also increases, which further leads to a higher initial temperature. As expected,

the transverse waveguide diameter increases with increasing net exposure, through the decreasing scan speed with increase in absorbed energy, lead to a larger waveguide diameter. This could be attributed to the strong heat diffusion effects owing to an increases photo-ionization rate.

#### 4. Discussion

As the input pulse energy increases the absorption in the focal spot increases as evident from the Fig. 3. The increase in absorption with respect to incident laser energies results in higher initial temperatures. This strong laser-induced temperature rise within the laser spot results in a molten volume which expands to sizes much larger than the spot size as further laser pulses are absorbed.

The temperature dependent specific heat, density and thermal diffusivity contribute to deviation between theory and experiment at the lower repetition rates, as room temperature values are considered in our modelling. The losses due to light scattering and laser induced plasma can also be accounted for discrepancies in the measured mode field diameter.

The waveguide diameter can be controlled and the desired single mode field diameter from 8.56 to 12.64  $\mu\text{m}$  can be acquired by proper choice of scan speed and pulse energy. Hence, the desired diffusion diameter between 6.125  $\mu\text{m}$  and 18.38  $\mu\text{m}$  can be tailored by adjusting the incident pulse energy from 623 nJ to 806 nJ and scan speed from 1 mm/s to 4 mm/s for writing single mode waveguides.

#### 5. Conclusion

In this paper, we detail the fabrication and characterization of a direct laser written waveguide in GeGaS. The mode field image of the waveguides and compared with the melt diameter derived using the heat diffusion model. The experimental results are found to match well with the theoretically calculated values.

#### Reference

- [1] B. J. Eggleton, B. L. Davies, K. Richardson, *Nature Photonics* **5**, 141 (2011).
- [2] C. D. Lezal.et.al, *J. Optoelectron. Adv. Mater.* **5**, 23 (2003).
- [3] A. Zakery, S. R. Elliott, *Springer Series in Optical Sciences*, (2007).
- [4] P. Nemec, B. Frumarova, M. Frumara, J. Oswald, *Journal of Physics and Chemistry of Solids*, **61**, 1583 (2000).
- [5] T. Sabapathy, A. Ayiriveetil, S. Asokan, A. K. Kar, S. J. Beecher, *Optical Materials Express* **2**, 1556 (2012).
- [6] J. R. Macdonald, R. R. Thomson, S. J. Beecher, N. D. Psaila, H. T. Bookey, A. K. Kar, *Opt. Lett.* **35**, 4036 (2010).
- [7] G. D. Valle, R. Osellame, N. Chiodo, S. Taccheo, G. Cerullo, P. Laporta, A. Killi, U. Morgner, M. Lederer, D. Kopf, *Opt. Express* **13**, 5976 (2005).
- [8] S. J. Beecher, R. R. Thomson, N. D. Psaila, Z. Sun, T. Hasan, A. G. Rozhin, A. C. Ferrari, A. K. Kar, *Appl. Phys. Lett.* **97**, 111114 (2010).
- [9] A. Ródenas, G. Martin, B. Arezki, N. D. Psaila, G. Jose, A. Jha, L. Labadie, P. Kern, A. K. Kar, R. Thomson, *Optics Letters*, **37**, 392 (2012).
- [10] G. Cerullo, R. Osellame, S. Taccheo, M. Marangoni, D. Polli, R. Ramponi, P. Laporta, S. De Silvestri, *Opt. Lett.* **27**, 1938 (2002).
- [11] Y. Cheng, K. Sugioka, K. Midorikawa, M. Masuda, K. Toyoda, M. Kawachi, K. Shihoyama, *Opt. Lett.* **28**, 55 (2003).
- [12] M. Ams, G. D. Marshall, D. J. Spence, M. J. Withford, *Opt. Express* **13**, 5676 (2005).
- [13] S. Ho, Y. Cheng, P. R. Herman, K. Sugioka, K. Midorikawa, *Technical Digest (CD) Optical Society of America*, Oxford, 2004.
- [14] R. R. Thomson, A. S. Bockelt, E. Ramsay, S. Beecher, A. H. Greenaway, A. K. Kar, D. T. Reid, *Opt. Express* **16**, 12786 (2008).
- [15] F. He, H. Xu, Y. Cheng, J. Ni, H. Xiong, Z. Xu, K. Sugioka, K. Midorikawa, *Opt. Lett.* **35**, 1106 (2010).
- [16] R. Osellame, S. Taccheo, M. Marangoni, R. Ramponi, P. Laporta, *J. Opt. Soc. Am. B.* **20**, 1559 (2003).
- [17] R. R. Thomson, A. S. Bockelt, E. Ramsay, S. Beecher, A. H. Greenaway, A. K. Kar, D. T. Reid, *Optics Exp.* **16**, 12786 (2008).
- [18] M. Shimizu, M. Sakakura, M. Ohnishi, *J. Appl. Phys.* **108**, 073533 (2010).
- [19] T. Sabapathy, M. S. R. N. Kiran, A. Ayiriveetil, A. K. Kar, U. Ramamurty, S. Asokan, *Opt. Mater. Express* **3**, 684 (2013).
- [20] R. R. Gattass, E. Mazur, *Nature Photonics* **2**, 219 (2008).
- [21] S. K. Sundaram, E. Mazur, *Nat. Materials* **1**, 217 (2002).
- [22] M. Sakakura, M. Shimizu, Y. Shimotsuma, K. Miura, K. Hirao, *Appl. Phys. Lett.* **93**, 231112 (2008).
- [23] E. A. Romanova, A. I. Konyukhov, *Optics and Spectroscopy* **104**, 784 (2008).
- [24] C. B. Schaffer, J. F. Garcia, E. Mazur, *Appl. Phys. A* **76**, 351 (2003).
- [25] J. W. Chan, T. R. Huser, S. H. Risbud, J. S. Hayden, D. M. Krol, *Appl. Phys. Lett.* **82**, 2371 (2003).
- [26] M. A. Hughes, W. Yang, *Journal of the Optical Society of America B* **26**, 1370 (2009).
- [27] S. M. Eaton, H. Zhang, P. R. Herman, F. Yoshino, L. Shah, J. Bovatsek, A. Y. Arai, *Opt. Express* **13**, 4708 (2005).
- [28] Y. Jaluria, K. E. Torrance, *Computational Heat Transfer*, Taylor & Francis, New York, 2003.
- [29] S. M. Eaton, H. Zhang, M. L. Ng, J. Li, W. J. Chen, S. Ho, P. R. Herman, *Opt. Express* **16**, 9443 (2008).

\*Corresponding author: sasokan@iap.iisc.ernet.in